Ethynyl and Ethenyl Ferrocenyl Dyads with Acridine, Acridone, and Anthraquinone

Elise M. McGale, Brian H. Robinson,* and Jim Simpson

Department of Chemistry, University of Otago, P.O. Box 56, Dunedin, New Zealand

Received September 10, 2002

Ethynylferrocenyl derivatives of 2,7-acridine (**1**, **2**), 9-*N*-acridone (**4**), and 2-anthraquinone (**6**) are described. (*Z*)-10-(2-iodo-1-ethenylferrocene)-9(10*H*)-acridinone (**3**), an intermediate in the formation of **4**, *N*-Fc$(CH_2)_n$-acridone (**5**; $n = 8$, 11), 1-Fc-anthraquinone (**7**), and (*E*)-(2-FcC═C)-anthraquinone (**8**) were also investigated. The X-ray structures of **3** and **6** were determined. B3LYP calculations, UV/vis spectroelectrochemistry, cyclic voltammetry, and ESR spectra were used to probe the ground and excited states of both the neutral and oxidized compounds. Emission is observed from oxidized, but not neutral, **4** and **6**; however, **1**, **2**, and **8** are fluorescent. Surprisingly, emission is reduced upon oxidation of **2** and **8**, which appears to correlate with the greater distortion in the excited compared to ground states.

Introduction

Photoactive donor-conjugated link-acceptor dyads are typically composites with a donor fluorophore and a suitable electron acceptor, or the reverse. If one component is redox active, each redox state may or may not interact with the photoexcited fluorophore through either an electron-transfer or an energy-transfer mechanism. Interest in the use of these dyads spans photovoltaic devices, fluorescent biological probes, molecular switches, and sensors.[1,2] As part of our program investigating durable, redox-mediated, organometallic fluorescent or electroluminescent materials, we have been taking advantage of the fast, reversible electron transfer of the $[Fc]^{+/0}$ couple while retaining the luminescent properties of the fluorophore. The well-known,[3,4] characteristic property of a ferrocenyl unit to act as a quencher of triplet states does militate against our goal. Nevertheless, numerous applications of both inter- and intramolecular quenching of triplet excited states have appeared.[4] Recently, a few neutral ferrocenyl derivatives which retain at least some emission of the parent fluorophore[5] or recover their fluorescence in the presence of ionophores[6] have been reported. Oxidation of a ferrocenyl assemblage to the ferrocenium ion in a conjugated system can block the electron-transfer mechanism with consequential increase in emission.[5a,7] On the other hand, quenching by a ferrocenium ion can also occur[8] and, in electroluminescent systems, recombination of charges generated at the electrode[9] or in an enzyme system can lead to excited-state emission.[10]

Recently, we have found[11] that the neutral electrophores [FcC═C] and [FcC≡C] fulfill the function of linking donors, and their oxidized counterparts $[FcC{=}C]^+$ and $[FcC{\equiv}C]^+$ act as linking acceptors, in dyads of the type polycyclic aromatic/unsaturated link/electrophore. Furthermore, the oxidized dyads were characterized by low-energy charge-transfer bands, some as low as 2400 nm (4170 cm^{-1}), the energy of which linearly correlated with the ionization energies and potentials for oxidation of the polycyclic aromatic donor. This prompted an investigation of molecules where the donor in the oxidized assemblage was a polycyclic *N*-heteroaromatic or quinone. Three classical fluorophores were chosen—acridine, acridone, and anthraquinone—to enable functionalization with an ethynylferrocenyl group attached at the hetero junction as well as at the π-aromatic ring. No ferrocenyl derivatives of acridine or acridone have been reported, although a ferrocenylacridine orange dye, an intercalant for DNA, has been described by Chen.[12] Nishihara and co-workers[13] have investigated several ethynylferrocenyl anthraquinone derivatives and shown that these compounds display unusual structural change and spin separation driven by the proton-coupled intramolecular electron transfer from ferrocene to the anthraquinone. Dyads analogous to those reported in this

* To whom correspondence should be addressed. E-mail: brobinson@alkali.otago.ac.nz.

(1) (a) Fabbrizzi, L.; Licchelli, M.; Pallavicini, P. *Acc. Chem. Res.* **1999**, *32*, 846−853. (b) Ward, M. D. *J. Chem. Educ.* **2001**, *78*, 321−328. (c) Bergonze, R.; Fabbrizzi, L.; Licchelli, M.; Mangano, C. *Coord. Chem. Rev.* **1998**, *170*, 31−46.

(2) De Silva, A. P.; Gunaratne, H. Q. N.; Habib-Jiwan, J.-L.; McCoy, C. P.; Rice, T. E.; Soumillion, J.-P. *Chem. Rev.* **1997**, *97*, 1515−1566.

(3) Geoffroy, G. L.; Wrighton, M. S. *Organometallic Photochemistry*; Academic Press: New York, 1969; Chapters 1−5.

(4) Fery-Forgues, S.; Delavaux-Nicot, B. *J. Photochem. Photobiol. A* **2000**, *132*, 137−159 and references therein.

(5) (a) Schmidt, E. S.; Calderwood, T. S.; Bruice, T. C. *Inorg. Chem.* **1986**, *25*, 3718−3720. (b) Rai, C. U.S. Patent 3,461,287, Aug 1969. (c) Delavaux-Nicot, B.; Fery-Forgues, S. *Eur. J. Inorg. Chem.* **1999**, *10*, 1821−1825.

(6) Beer, P. D.; Graydon, A. R.; Sutton, L. R. *Polyhedron* **1996**, *15*, 2457−2461. Beer, P. D.; Szemes, F.; Balzani, V.; Sala, C. M.; Drew, M. G. B.; Dent, S. W.; Maestri, M. *J. Am. Chem. Soc.* **1997**, *119*, 11864−11875.

(7) Wang, Z.; Kongchang, C.; Tian, H. *Chem. Lett.* **1999**, 423−424.

(8) Abruna, H. D. *J. Electrochem. Soc.* **1985**, *132*, 842−849.

(9) Schiffrin, D.; Wilson, R. PCT Int. Appl. WO 97 36931.

(10) Pragst, F.; Gruenberg, C.; Knaack, J.; Jugelt, W. *Z. Phys. Chem. (Leipzig)* **1974**, *255*, 696−710.

(11) Flood, A.; McAdam, C. J.; Gordon, K. C.; Hudson, R. D.; Manning, A. R.; Robinson, B. H.; Simpson, J. *J. Chem. Soc., Dalton Trans.*, submitted for publication.

(12) Chen, Y. *Huaxue Xuebao* **1993**, *51*, 308−312.

(13) Murata, M.; Takako, F.; Yamada, M.; Kurihara, M.; Nishihara, H. *Chem. Lett.* **2000**, 1328−1329. Murata, M.; Yamada, M.; Fujita, T.; Kojima, K.; Kurihari, M.; Kubo, K.; Kobayashi, Y.; Nishihara, H. *J. Am. Chem. Soc.* **2001**, *123*, 12903−12904.

10.1021/om020747t CCC: $25.00
Publication on Web 02/01/2003

Scheme 1

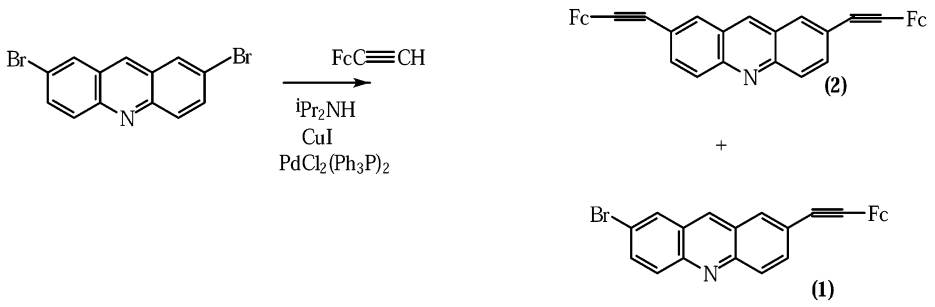

Scheme 2

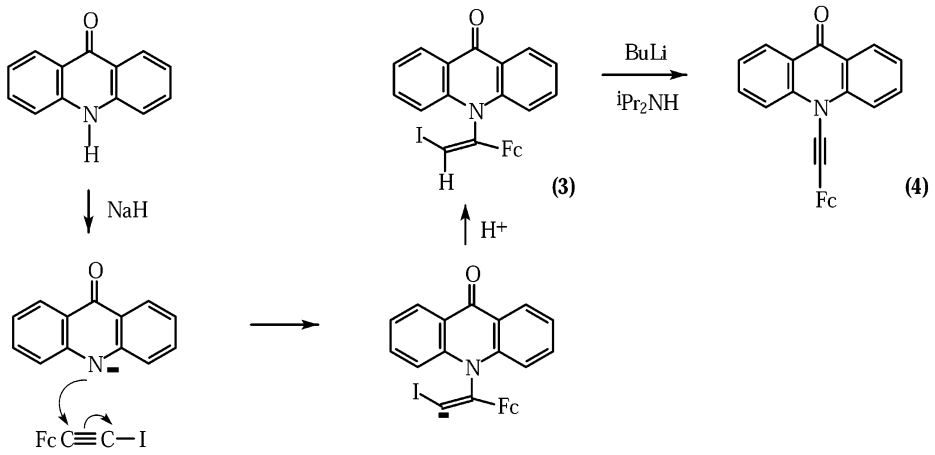

paper but with a cycloplatinated redox center are described elsewhere.[14]

Results and Discussion

Synthesis and Characterization. Sonogashira cross-coupling reactions of ethynylferrocene with 2,7 dibromoacridine gave 2-ethynylferrocene-7-bromoacridine (**1**) and 2,7-ethynylferroceneacridine (**2**), characterized by elemental analysis, ES-MS, and ^{1}H NMR and IR spectroscopy (Scheme 1). The relative yields of **1** and **2** could be controlled by varying the amount of ethynylferrocene, and they were easily separated, because **2** precipitated in CH_2Cl_2, whereas **1** eluted on silica gel.

9-(*N*-Alkynyl)acridinamines have been synthesized[15] via nucleophilic displacement reactions between 9-chloroacridine and *N*-alkynylamines, but this reaction was unsuccessful with ferrocenylamines.

In contrast to the acridine system, acridone dyads equivalent to **1** and **2** were not accessible (via Sonogashira coupling or Ullmann condensations), whereas N-linked derivatives were readily made. Deprotonation of acridone to the anion and nucleophilic attack on iodoethynylferrocene gave (*Z*)-10-(2-iodo-1-ethenylferrocene)-9(10H)-acridinone (**3**) instead of the expected ferrocenylynamine acridone (Scheme 2).

Similar β-adduct formation has been noted in nucleophilic substitution reactions of organic alkynes (e.g. bromoethynylbenzene[16a]), even when the alkyne is sterically congested (*tert*-butylchloroacetylene[16b]). The preference for nucleophilic substitution to form **3** can be explained by the α-iodine substituent stabilizing the developing negative charge. The ^{1}H NMR spectrum showed typical symmetrical acridone aromatic proton peaks in the region from 7.38 to 8.56 ppm, along with the olefinic proton peak at 7.48 ppm. An X-ray crystal structure gave the structural details for **3**. A perspective view is shown in Figure 1, which also defines the atom-numbering scheme. The structure of **3** comprises an acridone unit linked through the acridone nitrogen, N(1), to an alkene substituent. The acridone-bound

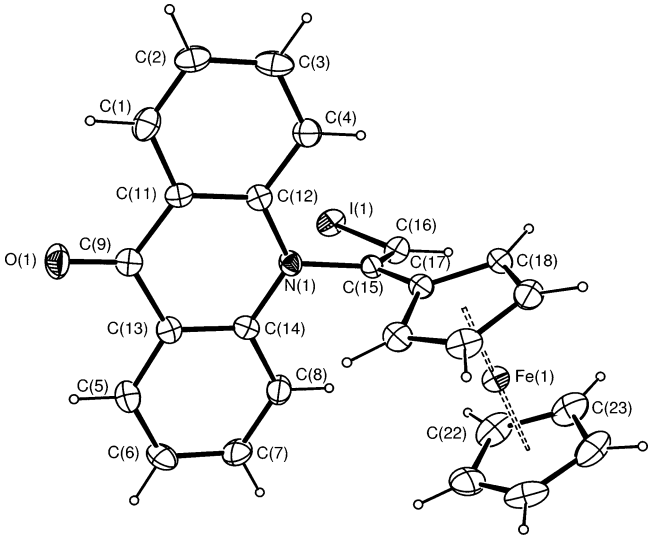

Figure 1. Perspective view of **3** showing the atom-numbering scheme, with displacement ellipsoids drawn at the 50% probability level. For clarity only two carbon atoms of the consecutively numbered cyclopentadienyl rings have been labeled.

(14) McGale, E. M.; Murray, E.; McAdam, C. J.; Morgan, J. L.; Robinson, B. H.; Simpson, J. *Inorg. Chim. Acta*, in press.
(15) Reisch, J.; Kamal, G. M.; Gunaherath, B. *J. Heterocycl. Chem.* **1993**, *30*, 1677−1678.
(16) (a) Katritzky, A. R.; Ramer, W. H. *J. Org. Chem.* **1985**, *50*, 855−856. (b) Viehe, H. G. *Angew. Chem., Int. Ed. Engl.* **1967**, *6*, 767−768.

Table 1. Selected Bond Lengths (Å) and Angles (deg) for 3

C(1)−C(2)	1.388(7)	C(6)−C(7)	1.360(7)
C(1)−C(11)	1.373(6)	C(7)−C(8)	1.384(6)
C(2)−C(3)	1.394(7)	C(8)−C(13)	1.370(7)
C(2)−C(15)	1.510(7)	C(13)−C(9)	1.485(7)
C(3)−C(4)	1.377(7)	C(9)−O(9)	1.206(6)
C(4)−C(12)	1.376(7)	C(9)−C(11)	1.477(7)
C(12)−C(11)	1.409(7)	C(15)−C(16)	0.947(6)
C(12)−C(10)	1.477(7)	C(16)−C(17)	1.527(7)
C(10)−O(10)	1.229(6)	C(17)−C(21) ring (av C−C)	1.41(3)
C(10)−C(14)	1.480(7)	C(22)−C(26) ring (av C−C)	1.400(13)
C(14)−C(5)	1.351(6)	Fe−C(17−21) (av)	2.039(13)
C(14)−C(13)	1.395(7)	Fe−C(22−26) (av)	2.039(16)
C(5)−C(6)	1.383(7)		
C(16)−C(15)−C(2)	178.7(7)	C(15)−C(16)−C(17)	175.2(6)

alkene C atom, C(15), also carries a ferrocenyl moiety with an iodo substituent, cis to the acridone, on the adjacent alkene carbon, C(16). The plane of the substituted cyclopentadiene ring C(17)- - -C(21) is inclined at an angle of 30.5(2)° to the best-fit plane of the alkene (C(15)C(16)C(17)N(1)I(1)), while the acridone unit is approximately orthogonal to this plane (86.52(7)°). The alkene group is reasonably planar with torsion angles N(1)−C(15)−C(16)−I(1) = −0.9(5)° and C(17)−C(15)−C(16)−I(1) = −178.1(3)°, indicating that steric interactions between the bulky substituents on C(15) are minimized. The acridone moiety adopts a characteristic "bent" shape with a dihedral angle between the planes subtended about the N(1)···C(9) vector of 3.1(2)°. In comparison to 1-(9-acridon-10-yl)-3,4,4-tricyano-1,3-butadiene, which has a butadiene substituent on the acridone N atom,[17a] bond distances and angles found within the acridone unit of **3** show some significant differences (Table 1). These are particularly marked in the vicinity of the acridone N atom. The N(1)−C(15) distance observed here, 1.454(5) Å, is significantly longer than the corresponding distance in the butadiene derivative, 1.367 Å, suggesting much less electron delocalization to the alkene unit in **3**. Indeed, data for the acridone unit in **3** are more comparable with those found for 9,10-dihydroxo-9-oxo-10-acridineacetic acid,[17b] where the possibility of delocalization is attenuated by the N-bound CH_2 group. It is likely that the steric demands of two bulky substituents on the C(15) atom in **3** have additional, electronic consequences in terms of delocalization in the molecule. The cyclopentadiene rings of the ferrocenyl substituent are partially eclipsed, with a mean C(m)−C(1g)−C(2g)−C(n) (m = 17−21; n = 22−26) torsion angle of 5(2)° and a dihedral angle between the Cp ring planes of 1.5(3)°. The average Fe−C distance, 2.048(5) Å, is not unusual, and the Fe(1) atom lies 1.655(2) and 1.649(2) Å, respectively, from the Cp ring planes. Molecules of **3** are reasonably well separated in the unit cell, with the shortest contact, not involving H atoms, being I(1)···O(1) (2.976(5) Å; $-^1/_2 + x$, $^1/_2 - y$, $-^1/_2 + z$). There is also evidence for weak, offset π-stacking between adjacent acridone units down the a axis (Figure 2a).

β-adducts such as **3** undergo α-elimination and an "onium" rearrangement to give acetylene derivatives,[18]

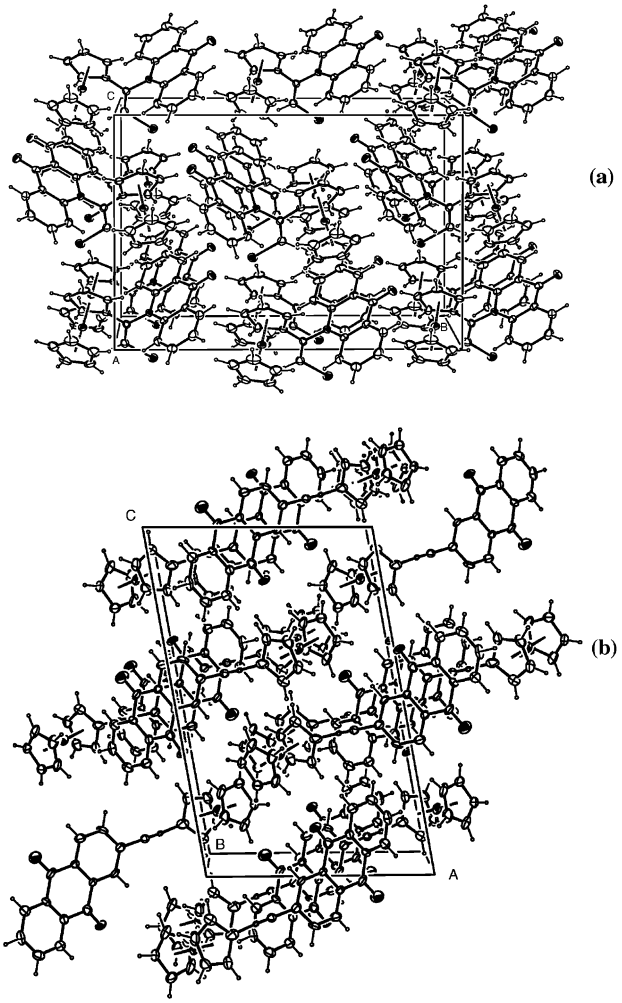

Figure 2. Packing diagrams for (a) **3** and (b) **6**.

Scheme 3

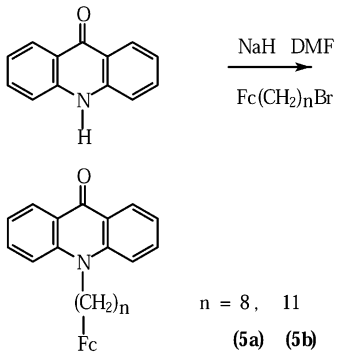

and this strategy was employed to form 10-(ethynylferrocene)-9(10*H*)-acridinone (**4**), using *n*-butyllithium as the base (Scheme 2). **4** was characterized by elemental analysis, ES-MS, and ^{1}H NMR and IR spectroscopy.

It was of interest to compare the effect of an insulated ferrocenyl redox unit in an *N*-acridone dyad with one that was part of an unsaturated linkage, as in **4**. This was achieved by the synthesis of 10-(8-ferrocenyloctyl)-9(10*H*)-acridinone (**5a**) and 10-(11-ferrocenylundecyl)-9(10*H*)-acridinone (**5b**) as air-stable yellow solids via the nucleophilic attack of the acridone anion on 8-bromooctyl- and undecylferrocene, respectively (Scheme 3).

Unlike acridone, ethynylferrocene dyads with anthraquinone attached at the 1- or 2-positions are accessible

(17) (a) Chetkina, L. A.; Kurov, G. N.; Dmitrieva, L. L. *Kristallografiya* **1995**, *40*, 669−671. (b) Bobrzynska, D.; Turowska-Tyrk, I. *Acta Crystallogr., Sect. C* **1997**, *53*, 238.

(18) Viehe, H. G.; Delavarenne, S. Y. *Chem. Ber.* **1970**, *103*, 1216−1224.

Scheme 4

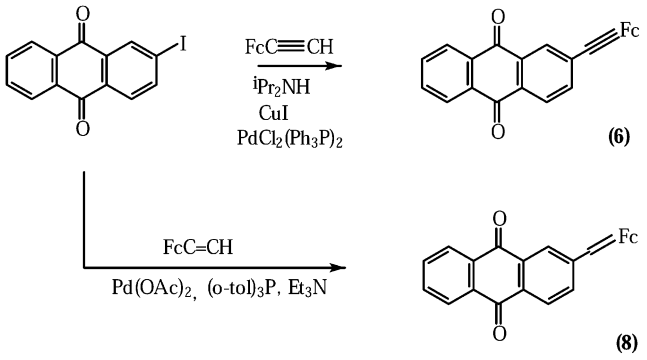

from the iodo- or aminoanthraquinone. Purple 2-ethynylferrocenylanthraquinone (**6**) was prepared in high yield by Sonogashira coupling of ethynylferrocene with iodoanthraquinone (Scheme 4) and characterized by elemental analysis, ES-MS, and ^{1}H NMR and IR spectroscopy. This compound has been briefly mentioned elsewhere.[13a] A perspective view from the X-ray structure of **6** and atom-numbering scheme are shown in Figure 3; selected bond lengths and angles are given in Table 2. The structure of **6** comprises an anthraquinone moiety, with an ethynylferrocene unit at the 2-position. To our knowledge, the only other structurally characterized alkyne-substituted anthraquinones have ethynylferrocene substituents in the 1-position[13a] and the 1,5- and 1,8-positions[13b] of the anthraquinone moiety. Regrettably, these reports give little or no structural information on the compounds for comparison purposes. For **6** the plane of the substituted cyclopentadiene ring C(17)−C(21) is inclined at an angle of 7.8(3)° to the best-fit plane of the anthraquinone moiety. This contrasts with the conformation observed for the 1-substituted analogue, where the anthraquinone and cyclopentadiene rings were approximately orthogonal; the corresponding details for the 1,5- and 1,8-derivatives are not reported. The positioning of the Fc and anthraquinone moieties, observed here, may facilitate the molecular packing of **6**, which occurs by way of interleaving head-to-tail stacks of the anthraquinone moieties down the *b* axis (Figure 2b). Bond distances and angles (Table 1) within the anthraquinone moiety show no significant differences from those observed in anthraquinone itself[19a] or in 2-methylanthraquinone.[19b] Difficulties with disorder within the alkyne moiety (see Experimental Section) preclude a detailed discussion of the evidence for alkyne-mediated delocalization between the anthraquinone and ferrocene moieties. The anthraquinone system is bent slightly about the C(9)···C(10) vector; the dihedral angle is 5.3(2)° between the planes defined by the atoms of the halves of the macrocycle (C(1)···C(4), C(9)···C(12) and C(5)−C(8), C(9), C(10), C(13), C(14)). The cyclopentadiene rings of the ferrocene substituent are not fully eclipsed, with the mean C(*m*)−C(1g)−C(2g)−C(*n*) (*m* = 17−21; *n* = 22−26) torsion angle being −16.3(8)° and the dihedral angle between the Cp ring planes being 4.5(4)°. The average Fe−C distance, 2.04(1) Å, is not unusual, and the Fe(1) atom lies 1.653(3) and 1.645(3) Å, respectively, from the Cp ring planes.

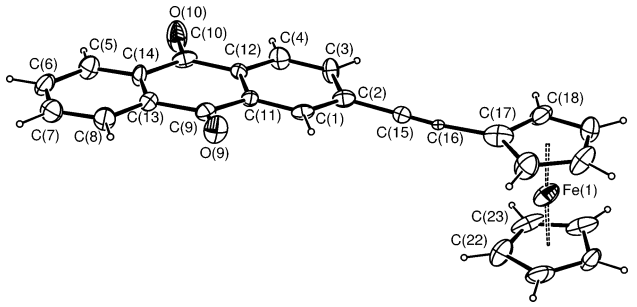

Figure 3. Perspective view of **6** showing the atom-numbering scheme, with displacement ellipsoids drawn at the 50% probability level. For clarity only two C atoms of the consecutively numbered cyclopentadienyl rings have been labeled.

Table 2. Selected Bond Lengths (Å) and Angles (deg) for 6

C(1)−C(2)	1.366(6)	C(11)−C(12)	1.412(5)
C(1)−C(11)	1.418(5)	C(12)−N(1)	1.402(5)
C(2)−C(3)	1.399(6)	C(13)−C(14)	1.401(5)
C(3)−C(4)	1.389(5)	C(14)−N(1)	1.399(5)
C(4)−C(12)	1.410(5)	N(1)−C(15)	1.454(5)
C(5)−C(6)	1.368(5)	C(15)−C(16)	1.339(5)
C(5)−C(13)	1.408(5)	C(15)−C(17)	1.468(5)
C(6)−C(7)	1.394(6)	C(16)−I(1)	2.079(4)
C(7)−C(8)	1.370(6)	C(17)−C(21) ring (av C−C)	1.429(5)
C(8)−C(14)	1.411(5)	C(22)−C(26) ring (av C−C)	1.416(7)
C(9)−O(1)	1.233(4)	Fe−C(17−21) (av)	2.048(6)
C(9)−C(11)	1.466(5)	Fe−C(22−26) (av)	2.047(3)
C(9)−C(13)	1.482(5)		
C(16)−C(15)−N(1)	120.1(3)	N(1)−C(15)−C(17)	114.7(3)
C(16)−C(15)−C(17)	125.2(3)	C(15)−C(16)−I(1)	124.1(3)

While the emphasis in this paper is ethynyl dyads, it was of interest to compare their excited-state chemistry with compounds where the energy transfer to a ferrocenyl group is via an ethene link or a direct bond to the fluorophore. Accordingly, two previously reported anthraquinone compounds, 1-ferrocenylanthraquinone[20] (**7**) and (*E*)-2-ethenylferrocenylanthraquinone[21] (**8**), obtained by a Heck coupling reaction, were also investigated.

Two spectroscopic parameters of **1**−**6**, δ(ferrocenyl) and ν(C≡C), could reflect the communication between the fluorophore acceptor and the ferrocenyl group. In ethynylferrocene, the ferrocenyl ^{1}H resonances occur at 4.22 (Cp), 4.20 (α, 2H), and 4.46 ppm (*β*, 2H). In **1**, **2**, and **6** the protons are shifted slightly downfield from these values (reversing the α and Cp sequence), which could be interpreted as a consequence of the acceptor capability of the fluorophores. However, the dyads with weaker acceptors display an even larger downfield shift; for example, δ(α) is 4.57 ppm for **6** and 4.65 ppm in the dyad FcC≡C-anthracene.[11] Furthermore, the ferrocenyl chemical shifts for the anthracene dyad and **4** are the same. The conclusion is that the ferrocenyl chemical shifts do not reflect the acceptor strength of the fluorophore but are dependent on the point of attachment. The same conclusion is reached from an examination of ν(C≡C). These energies are essentially the same (2208 ± 1 cm^{-1}) when the FcC≡C group is bound to the aromatic ring (**1**, **2**, **6**), irrespective of the type of fluorophore in the dyad; they are also similar to ν(C≡C)

(19) (a) Fu, Y.; Brock, C. P. *Acta Crystallogr., Sect. B* **1998**, *54*, 308−315. (b) Kingsford-Adaboh, R.; Kashino, S. *Acta Crystallogr., Sect. C* **1995**, *51*, 2094−2096.

(20) Roberts, R. M. G. *J. Organomet. Chem.* **1990**, *388*, 181−186.
(21) Liu, S.-G.; Perez, I.; Ignacio, M. N.; Echegoyen, L. *J. Org. Chem.* **2000**, *65*, 9092−9102.

Table 3. $E^{0/+}$, UV−Vis, and Emission Data[a]

		UV−vis			emission[e]	
	$E^{0/+}$	neutral	oxidized[b]	CT band[d]	neutral	oxidized
1	0.68	314 *(31)*, 380 (*8.7*), 460[c] *(1.8)*	380 (*13*), 440[c] (*6.9*)	840	390, *420*	375, *500*
2	0.67	324 (*28*), 383 (*10*), 470[c] (*6.4*)	411 (*17.7*), 592 (*8.2*)	843	350, *420*[g]	390, *515*
3	0.76	391(*12*), 473 *(0.66)*				
4	0.70	389 (*4.3*)	375 (*7.7*), 453 (*3.7*)	934		390, *425*
5a/5b	0.49	382 (5.7), 401 (*6.1*)	380 (*5.7*), 400 (*6.1*)	630	390, *410*	390, *410*
6	0.71	360 (*6.9*), 516 (*1.7*)	365,[c] 430,[c] 516	757		390, *425*
7	0.60	366 (*7.5*), 524 (*2.1*)	386, 630		388, *425*[f]	501, *582*
8	*0.53*	314 (*21*), 369 (*11.5*), 543 (*3.4*)	360 (12.4)	909	396, *494*[g]	400, *545*

[a] All data in CH_2Cl_2 at 20 °C. $E^{0/+}$ data: cyclic voltammetry, Pt, 200 mV s^{-1} in V, referenced against decamethylferrocene. UV−vis: λ_{max}/nm, $\epsilon/10^{-2}$ L mol^{-1} cm^{-1} (given in italics in parentheses), high-energy bands >300 nm not given. [b] From OTTLE experiments; intensities approximated from absorbance of neutral species. [c] Shoulder. [d] Equivalent band in naphthalene and anthracene dyads, respectively:[11] 873, 1118 (FcC≡C); 956, 1051 nm (FcC═C). [e] Excitation λ_{max}/nm and emission λ_{max}/nm (given in italics), taken from center of vibrational structure. Oxidized species produced by controlled electrolysis. [f] Very weak. [g] In MeCN: **2**, 425, *490*; **8**, 435, *556*.

in polyaromatic dyads (e.g. 2203 cm^{-1} for FcC≡C-anthracene).[11] There is a significant difference in ν(C≡C) between **4** (2224 cm^{-1}) and **2** and **6**, which undoubtedly reflects the fact that **4** is an ynamine.

Electronic Spectra. UV−vis data are given in Table 3. In general, there is a small red shift in energy of the $\pi-\pi^*$ or n−π^* bands relative to the respective parent fluorophore and an increase in intensity where there is an ethynyl linkage. Likewise, the energy of the "low energy"[22] ferrocenyl band in the acridine and acridone compounds is similar to that for FcC≡CH; it is often a shoulder on the fluorophore bands, and this makes intensity measurements difficult. These data indicate that there is little perturbation of the fluorophore by the redox center: that is, weak communication between the donor and acceptor in the ground state of the neutral molecules. On the other hand, there is a significant red shift (3400−3100 cm^{-1}) in this "low energy" ferrocenyl transition for the anthraquinone compounds **6**−**8** and an order of magnitude increase in intensity (note that the intensity for **8** is ∼2× that for **6**). Both the red shift and increased intensity suggest some degree of communication between the two components of the dyads, especially in **8**. In view of the difference in PCET behavior between the 1- and 2-substituted anthraquinones, it is interesting that 1-ethynylanthraquinone[13] and **6** and **8** have the same energy for the ferrocenyl transitions.

To assist in defining the frontier orbitals involved in these transitions, B3LYP calculations were carried out for the ethynyl dyads. Three conclusions could be drawn from these calculations. First, whereas the HOMO of the 2-anthraquinone compounds has considerable ethynyl character (cf. anthraquinone itself, where the electron density is centered on the quinoidal framework), there is little ethynyl character in the HOMO of the 2-acridine and acridone compounds. Second, the LUMO/excited state of all the compounds has a much smaller contribution from the ethynyl link than the HOMO, and it is essentially a fluorophore orbital. The N and CO contribution to the LUMO increases as the number of CO groups in the organic component increases. Third, there is a symmetry mismatch between the FcC≡C− link and the fluorophore, irrespective of the point of attachment. A similar mismatch exists within FcC≡C-aryl dyads.[23] Thus, the UV−vis data and calculations are consistent and support the difference between the anthraquinone and acridine/acridone dyads, a difference that is a ground-state HOMO effect. An MLCT description of the "low-energy" ferrocenyl band for **6**−**8** is reasonable, but the transition is localized on the ferrocenyl component for the acridine and acridone dyads.

Spectroelectrochemistry. To probe the ground and excited states further, the spectroelectrochemistry of **1**, **2**, and **4**−**8** was investigated; **3** was not studied in detail, as the products of oxidation proved unstable. All the compounds displayed the normal, cyclic, and square-wave voltammograms in CH_2Cl_2 of a chemically reversible, one-electron, $[Fc]^{+/0}$ couple. Interesting trends can be seen in $[Fc]^{+/0}$ (Table 3, potentials referenced against the solvent-independent $[Fc^*]^{+/0}$ couple). An ethynyl substituent on a ferrocenyl ring is an electron-withdrawing group, as shown by the anodic shift: $[FcC{\equiv}CH]^{+/0} = 0.71$ V compared to $[FcH]^{+/0} = 0.55$ V. Potentials for all the ethynyl dyads **1**, **2**, **4**, and **6** are essentially the same as for FcC≡CH; similarly, $[\mathbf{8}]^{+/0} \cong [FcC{=}CH]^{+/0}$ (0.52 V). That is, the π-conjugated link isolates, in the ground state, the ferrocenyl couple from the effect of being incorporated in a dyad with a strong acceptor, irrespective of whether it is N-bonded or directly linked to the aromatic ring. This is a consequence of the orbital mismatch noted above. A more dramatic illustration of the mismatch effect is that $[\mathbf{7}]^{+/0}$ is only slightly anodic of $[FcH]^{+/0}$, even though the ferrocenyl group is directly bound to the acceptor. As expected, the distance and electron-donating effect of the long-chain saturated link ensures that $[\mathbf{5a}]^{+/0}$ and $[\mathbf{5b}]^{+/0}$ (0.49 V) are cathodic of $[FcH]^{+/0}$ (0.55 V). The most anodic potential, that of $[\mathbf{3}]^{+/0}$, is attributed to the extra electron-withdrawing effect of the trans iodine substituent.

Irreversible reduction to the radical anions of the dyads was observed at potentials <−1.00 V. ESR studies were carried out on the radical anions $\mathbf{2}^{\bullet-}$ and $\mathbf{4}^{\bullet-}$ produced in situ by electrochemical reduction at low temperatures at −1.1 V. These weak radical anion spectra (the spectrum for $\mathbf{4}^{\bullet-}$, g value and hyperfine constant are given in Figure 4) were indistinguishable from those produced from the parent fluorophores by the same technique and from data in the literature.[24] Clearly, the LUMO in the neutral species and SOMO

(22) Barlow, S.; Marder, S. R. *Chem. Commun.* **2000**, 1555−1562.
(23) Weyland, T.; Costuas, K.; Mari, A.; Halet, J.-F.; Lapinte, C. *Organometallics* **1998**, *17*, 5569−5579.
(24) Gerson, F. *High-Resolution ESR Spectroscopy*; Wiley: New York, 1970.

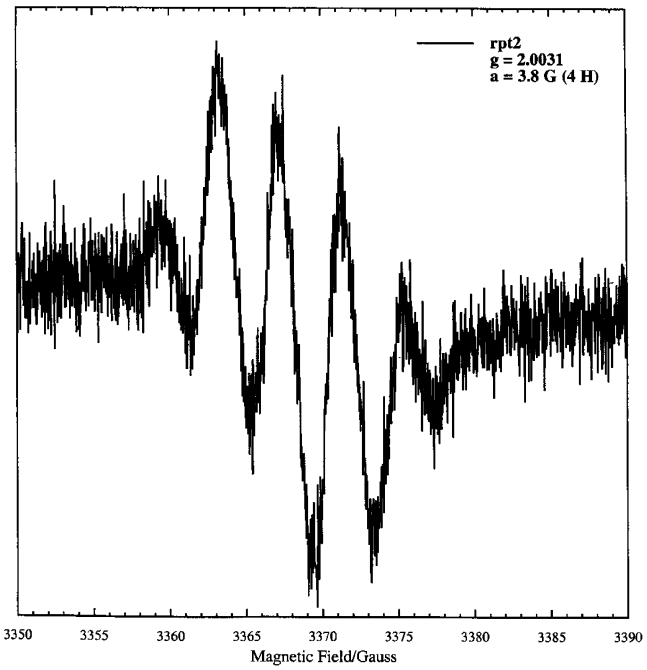

Figure 4. ESR spectrum of $\mathbf{4}^{\bullet-}$ in CH_2Cl_2 at 20 °C generated by in situ electrolysis at −1.1 V.

in the reduced species are centered on the fluorophore, as predicted from the B3LYP calculations.

Each compound was oxidized in situ to the cations at the appropriate $[Fc]^{+/0}$ potential in UV−vis OTTLE (Pt electrode) cells in CH_2Cl_2; the spectra of the final oxidation products were also obtained by chemical oxidation and electrolysis. Consistent isosbestic points and complete reversibility when the potential was cycled in the OTTLE experiment attest to the stability of these cations. For the system with a saturated link to the acridone, **5a** and **5b**, the energies of the fluorophore transitions for the neutral and oxidized species were identical, while the "low-energy" ferrocenyl transition at 401 nm is replaced by a band at 630 nm in $\mathbf{5a}^+$ and $\mathbf{5b}^+$, giving the typical green color of the ferrocenium cation. Thus, the energy levels of the acridone are unperturbed by either a Fc or Fc^+ unit.

In contrast, the formation of compounds $\mathbf{1}^+$, $\mathbf{2}^+$, $\mathbf{4}^+$, and $\mathbf{6}^+$−$\mathbf{8}^+$ gave rise to spectra with a new band profile (a representative OTTLE spectrum, that for **1**, is given in Figure 5). The most important feature of these OTTLE spectra was that all unsaturated-linked dyads displayed broad ($\Delta\nu_{1/2} \approx 4 \times 10^3$ cm^{-1}) bands between 750 and 950 nm upon oxidation (Table 3). A dependence of the energy of these bands on the donor capability of the fluorophore and the solvatochromism are consistent with a fluorophore (donor) → ferrocene (acceptor) charge-transfer transition. A large negative solvatochromic shift of ∼1000 cm^{-1} on going from CH_2Cl_2 to MeCN is indicative of a dipole in the ground state of the cation larger than that of the excited state. This is consistent with the CT assignment, as the excited-state configuration of the cations would have the positive charge delocalized over the dyad; in the ground state it is localized on the ferrocenyl acceptor. It is interesting that the CT band for the proton-coupled species from 1-ethynylferroceneanthraquinone (939 nm), which has a cumulene link between the donor and acceptor,[12a] is at a lower energy than that for **6** (757 nm), suggestive of

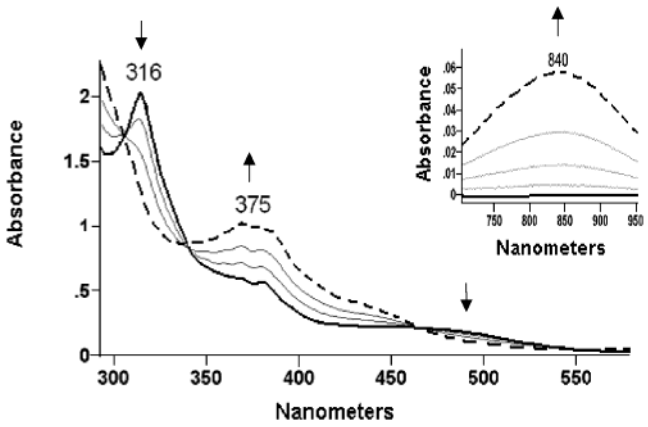

Figure 5. UV−vis OTTLE spectrum of **1** (20 °C, in CH_2Cl_2, Pt electrode, 0.7 V).

a stronger interaction in the former species. Low-energy transitions attributed to ligand → "Fe" charge transfer have been reported for a number of ferrocenium salts[25] and TCNE/TCNQ complexes,[26] and recently, we found that the CT bands in FcC≡C− or FcC═C− cyclic polyaromatic dyads linearly correlated with the ionization potential of the polyaromatic.[11] It is more difficult to formally correlate the CT energies for $\mathbf{1}^+$−$\mathbf{8}^+$, as the donor orbitals have different contributions from the hetero and FcC≡C groups. Nevertheless, the lower energy for $\mathbf{1}^+$ and $\mathbf{2}^+$ compared to $\mathbf{6}^+$ is consistent with the higher excitation energy (i.e. better donor ability) of acridine. It is interesting that the CT energy for the acridine dyads is similar to that for the FcC≡C-phenanthrene dyad,[11] as both donors have the same ionization potential: further evidence for the charge-transfer character of these low-energy bands. $\mathbf{4}^+$, where the donor is linked as an ynamine, via a donor nitrogen, has the lowest CT energy despite the IP of acridone (7.6 eV) being very similar to that of acridine (7.9 eV);[26] the calculations were in agreement with more effective communication in the ynamine. Excitation via an ethene link is more effective, as shown by a comparison between the CT energies of $\mathbf{6}^+$ and $\mathbf{8}^+$ (Table 3), an observation in accord with cyclic polyaromatic dyads.[11] From this perspective $\mathbf{4}^+$ is more like an enamine. The surprising result was that no CT bands were observed in the spectrum of $\mathbf{7}^+$. The ferrocenyl band at 542 nm was bleached on oxidation, and there was a suggestion of a very weak band at 630 nm, typical of a ferrocenium cation. This emphasizes the role of the unsaturated link.

There is no consistent pattern in the changes to the higher energy spectral profile of the neutral derivatives upon oxidation (Table 3). The band energies for the two acridine cations $\mathbf{1}^+$ and $\mathbf{2}^+$ are the same, with bleaching of the ferrocenyl HOMO/LUMO transition at 470 nm in **1** and **2** upon oxidation and the appearance of a shoulder at ∼440 nm (Figure 5). The similarity of these acridine spectra has a bearing on their emission behavior (vide infra). An increase in the intensity of the HOMO(SOMO)−LUMO ferrocenyl transition at 515 nm occurs from **6** to $\mathbf{6}^+$, as is observed upon the formation

(25) (a) Toma, S.; Gaplovsky, A.; Hudecek, M.; Langfelderova, Z. *Monatsh. Chemie* **1985**, *116*, 357−364. (b) Mendiratta, A.; Barlow, S.; Day, M. W.; Marder, S. R. *Organometallics* **1999**, *18*, 454−456.

(26) (a) Balestieri, F.; Franco, M. A.; Sabbatini, M. *Inorg. Chim. Acta* **1981**, *54*, L29−L30. (b) Rosenblum, M.; Fish, R. W.; Bennett, C. *J. Am. Chem. Soc.* **1964**, *86*, 5166−5170.

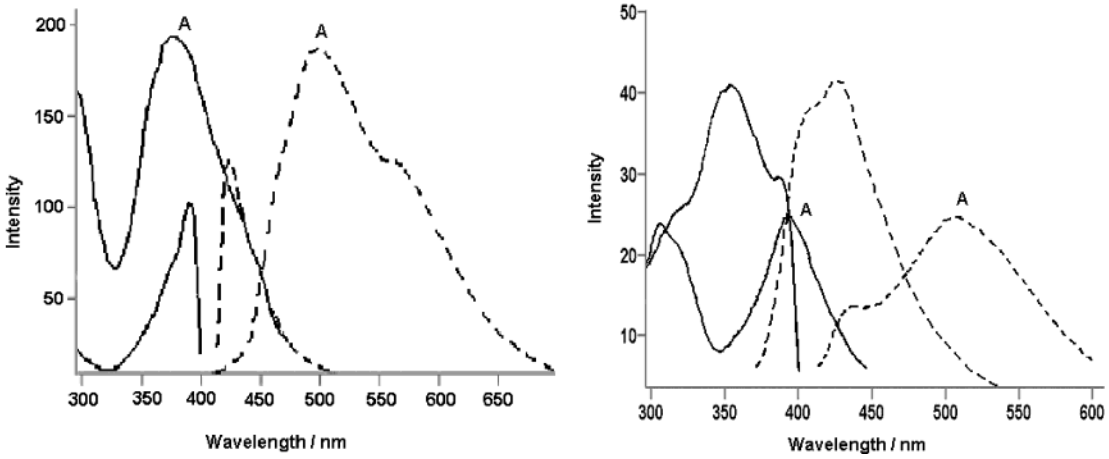

Figure 6. Emission spectra of (a) **1**/**1**$^+$ (b) **2**/**2**$^+$ at 20 °C in CH_2Cl_2: (—) excitation; (- - -) emission. A denotes the *oxidized* species.

of the 1-cumulene compound.[13a] On the other hand, the equivalent band at 524 nm in **7** is bleached, as is that for **8**. **5** and **5**$^+$ have the same profile, whereas oxidation of the ynamine **4** creates two new bands; this is in contrast to the case for the analogous cycloplatinated ynamine {*N*-Pt[(η^5-Cp)Fe(σ:η^5-$C_5H_3CH_2NMe_2$)](dmso)-(C≡C-acridone)}, where there is no change upon oxidation of the complex.[14]

Emission Spectra. A preliminary investigation of the emission spectra for the neutral and oxidized ethynyl dyads was undertaken (Table 3). Emission was essentially quenched in **4**, **6**, and **7** and partially quenched in **5** and **8**, but there was still significant emission from the acridine compounds. The emission from the neutral acridine compounds is the most intense observed from a polycyclic aromatic-fluorophore ferrocenyl dyad. In CH_2Cl_2, the Stokes shift for **2** was much larger (4800 cm^{-1}) than that for **1**, despite the similarity of the electronic spectra of **1** and **2**, and about the same as that for **8** (4950 cm^{-1}); for both **2** and **8** there is a strong solvent dependence on the λ_{max}(emission) value. The large Stokes shift and solvent effect indicate that the ground and excited states in these dyads have considerably different configurations, and a surprising consequence of this distortion for **2** and **8** appears to be that the emission behavior upon oxidation is anomalous (vide infra). A "distance effect", noted also in the emission of ferrocenylnaphthalimide derivatives[28] and the acridine orange compound reported by Chen,[12] is responsible for the residual emission from **5**. Moreover, the small Stokes shift of 1200 cm^{-1} shows that the ground and excited states are similar and it is essentially an "acridone" emission.

Inhibition of the electron-transfer mechanism caused an enhancement of fluorescence upon oxidation, and the emission spectra for **1**$^+$ and **4**$^+$—**7**$^+$ showed a considerable red shift in λ_{max} (Table 3 and Figure 6). The Stokes shifts for **5** and **5**$^+$ are identical, reinforcing the view that it is an acridone emission. Perturbation of the excited state is more evident in the other molecules, and the Stokes shift increases in the order **5**$^+$ = **6**$^+$ < **7**$^+$ ≪ **1**$^+$ (Table 3). That is, there is distortion of the excited state relative to the ground state in the oxidized acridine compounds, as in the neutral species, whereas the emission from the other oxidized dyads is largely from the unperturbed fluorophore. The **2**—**2**$^+$ and **8**—**8**$^+$ dyad systems were anomalous and novel in comparison with the emission from other ferrocenyl systems.[4] Emission is *reduced* upon oxidation. While the Stokes shifts are similar in both **2** and **2**$^+$, the shift is larger for **8**$^+$ than for **8**. What actually drives this reversal of emissive properties is uncertain at this time, and more detailed studies of other ethenylferrocenyl and disubstituted acridine dyads are underway.

Conclusion

The synthesis of ferrocenyl dyads of polycyclic N-aromatic and quinone fluorophores has given a valuable insight into the parameters required for the construction of emissive arrays with traditional dye molecules and point to deficiencies in our understanding of the factors that influence the excited-state configurations. There is little evidence for significant donor—acceptor communication, via an unsaturated link, in the ground or excited states of the neutral dyads. In the oxidized dyads the ferrocenium moiety is now the acceptor in the excited state, and new energy levels are created which provide low-energy charge transitions. This observation is important for NLO development and, if the intensity can be increased by better charge separation, for near-IR optical devices. Apart from **1**, **2**, and **8** the dyads follow the accepted pattern of quenched emission in the neutral species and restored emission in the oxidized species representing a molecular switch. A "distance effect" does sustain emission when the proximal ferrocenyl group is unable to swivel around to lie close to the fluorophore (as in **5b**). An explanation for the appreciable emission in **1** and **2**, and the surprising decrease of emission for **2** → **2**$^+$ and **8** → **8**$^+$, may be found in the significant contributions of FcC≡C or FcC═C to the excited-state configurations of **1** and **8**, respectively, compared to **4** or **6**. Detailed emission data are needed to elucidate the emission mechanisms.

Experimental Section

Solvents were dried and distilled by standard procedures. Commercial reagents were used as received. Ethynylferro-

(27) Votyuk, A. A.; Zerner, M. C.; Rosch, N. *J. Phys. Chem.* **1999**, *103*, 4553—4559.
(28) McAdam, C. J.; Robinson, B. H.; Simpson, J. *Organometallics* **2000**, *19*, 3644—3653.

cene,[29] iodoethynylferrocene,[30] 10-(2-propynyl)-9-acridone,[16] 2-iodoacridone,[31] 2,7-dibromoacridine,[31] (11-bromoundecyl)-ferrocene,[32] and (8-bromooctyl)ferrocene,[32] were prepared by literature procedures. Microanalyses were carried out by the Campbell Microanalytical Laboratory, University of Otago. ^{1}H NMR were recorded on a Varian Unity Inova 300 MHz spectrometer, IR on a Perkin-Elmer BX FT-IR instrument, UV−vis on a Varian Cary 500 scanning UV−vis−near-IR spectrophotometer, emission on a Perkin-Elmer LS 50B instrument, and ES-MS on a Schimadzu LCMS-QP8000 quadrople mass spectrometer. Ab initio calculations were performed by DFT methods using Gaussian 98 software;[33] the basis set was 6-31G(d). Molecular orbital contour plots were prepared by importing the Gaussian 98 output files into MOLDEN.[34] Cyclic voltammetry in CH_2Cl_2 and acetone were performed using a three-electrode cell with a polished Pt disk as the working electrode; solutions were $\sim 10^{-3}$ M in electroactive material and 0.1 M in supporting electrolyte (triply recrystallized $TBAPF_6$). Data were recorded on Powerlab/4sp electrochemical equipment. Scan rates of 0.1−2 V s^{-1} were typically employed. All potentials are referenced to decamethylferrocene. OTTLE cells were home-built with platinum electrodes for both IR and UV−vis spectroscopy.

Preparation of 2-Bromo-7-ethynylferroceneacridine (1) and 2,7-Diethynylferroceneacridine (2). A solution containing 2,7-dibromoacridine (53 mg, 0.16 mmol), ethynylferrocene (67 mg, 0.2 mmol), and 2 mol % $PdCl_2(Ph_3P)_2$/CuI in diisopropylamine (15 mL) was heated under reflux for 15 h. The reaction mixture was then extracted into CH_2Cl_2, and the extracts were washed with water and treated with $MgSO_4$. Column chromatography (CH_2Cl_2) eluted crude **1** as the second band, which was further purified using preparative silica plates (hexane−CH_2Cl_2−EtOAc) to give pure **1** (46 mg, 61%). Anal. Calcd for $C_{25}H_{16}NFeBr$: C, 64.41; H, 3.46; N, 3.01. Found: C, 64.32; H, 4.03; N, 2.53. ES-MS: *m*/*z* 466 (M^+). ^{1}H NMR ($CDCl_3$, δ): 4.29 (s, 5*H*, η^5-C_5H_5), 4.31 (t, 2*H*, *J* = 1.8 Hz, η^5-C_5H_4), 4.57 (t, 2*H*, *J* = 1.8 Hz, η^5-C_5H_4), 7.79−7.86 (m, 2*H*, acridine *H*), 8.07−8.18 (m, 4*H*, acridine *H*), 8.61 (t, 1*H*, *J* = 7.2 Hz, acridine *H*). IR (CH_2Cl_2, cm^{-1}): 2208 (ν(C≡C)). $E^{+/0}$ (CH_2Cl_2, V): 0.68. In a similar reaction, but with a 1:2 ratio of 2,7-dibromoacridine to ethynylferrocene, the solvent was removed in vacuo, CH_2Cl_2 added to the residue, and the bright red precipitate of **2** collected (0.421 g, 36%). ES-MS: *m*/*z* 596 (M^+). ^{1}H NMR ($CDCl_3$, δ): 4.29 (s, 10*H*, η^5-C_5H_5), 4.30 (t, 4*H*, *J* = 1.8 Hz, η^5-C_5H_4), 4.58 (t, 4*H*, *J* = 1.8 Hz, η^5-C_5H_4), 7.99 (dd, 3*H*, *J* = 9, 1.5 Hz, acridine *H*), 8.13−8.17 (m, 4*H*, acridine *H*), 8.65 (s, 1*H*, acridine *H*). IR (CH_2Cl_2, cm^{-1}): 2208 (ν(C≡C)). $E^{+/0}$ (CH_2Cl_2, V): 0.67. Workup of the filtrate as above gave **1** (0.240 g, 26%).

Preparation of (*Z*)-10-(2-Iodo-1-ethenylferrocene)-9(10*H*)-acridinone (3). Sodium hydride (0.04 g, 1 mmol) was added to a stirred solution of 9(10*H*)-acridone (0.20 g, 1 mmol) in dry DMF (5 mL) and the solution stirred for 30 min at 50 °C. Iodoethynylferrocene (0.48 g, 1.7 mmol) was then added and the reaction mixture stirred for a further 5 h. The solvent was removed in vacuo, the yellow residue taken up in CH_2Cl_2, and the solution washed with water and treated with $MgSO_4$. The CH_2Cl_2 extracts were concentrated and purified by chromatography on activated alumina. The first band was removed with CH_2Cl_2, and then **3** was eluted with EtOAc. Recrystallization in CH_2Cl_2/pentane gave 0.24 g (45%) of **3** as a dark red solid. Anal. Calcd for $C_{25}H_{18}ONFeI$: C, 56.53; H, 3.42; N, 2.64. Found: C, 56.81; H, 3.49; N, 2.77. ES-MS: *m*/*z* 532 (M^+). ^{1}H NMR ($CDCl_3$, δ): 4.10 (s, 5*H*, η^5-C_5H_5), 4.16 (t, 2*H*, *J* = 2 Hz, η^5-C_5H_4), 4.26 (t, 2*H*, *J* = 2 Hz, η^5-C_5H_4), 7.33 (ddd, 2*H*, *J* = 15, 9.5, 1 Hz, acridone *H*), 7.46 (dd, 2*H*, *J* = 10, 0.5 Hz, acridone *H*), 7.48 (s, 1*H*, −C=C*H*), 7.67 (ddd, 2*H*, *J* = 17, 10, 1.5 Hz, acridone *H*), *8*.60 (dd, 2*H*, *J* = 10, 0.5 Hz, acridone *H*). IR (CH_2Cl_2, cm^{-1}): 1636, 1606 (ν(CO), ν(NC)). $E^{+/0}$ (CH_2Cl_2, V): 0.76.

Preparation of 10-(Ethynylferrocene)-9(10*H*)-acridinone (4). Butyllithium (2 mL) and diisopropylamine (0.33 mL) were added to diethyl ether (5 mL) and cooled to −80 °C. **3** (90 mg, 0.17 mmol) in diethyl ether (5 mL) was added to the stirred reaction mixture and the temperature brought to room temperature. Solvent was removed in vacuo, the solid taken up in CH_2Cl_2, and the brown residue washed with CH_2Cl_2 until the washings were clear. The solvent was stripped and the crude product chromatographed on silica gel (CH_2Cl_2). The material from the first yellow band was further purified on preparative silica plates (2:1 hexane−CH_2Cl_2); the third band yielded pure **4** (40 mg, 59%). Anal. Calcd for $C_{25}H_{17}ONFe$: C, 74.46; H, 4.25; N, 3.47. Found: C, 73.95; H, 4.45; N, 3.52. ES-MS: *m*/*z* 403 (M^+). ^{1}H NMR ($CDCl_3$, δ): 4.36 (s, 5*H*, η^5-C_5H_5), 4.37 (t, 2*H*, *J* = 2 Hz, η^5-C_5H_4), 4.64 (t, 2*H*, *J* = 2 Hz, η^5-C_5H_4), 7.42 (ddd, 2*H*, *J* = 16.2, 9, 1.2 Hz, acridone *H*), 7.81 (ddd, 2*H*, *J* = 17.4, 10.2, 1.8, acridone *H*), 8.09 (d, 2*H*, *J* = 9 Hz, acridone *H*), 8.52 (dd, 2*H*, *J* = 9.3, 1.2 Hz, acridone *H*). IR (CH_2Cl_2, cm^{-1}): 2244 (ν(C≡C)), 1645, 1607. $E^{+/0}$ (CH_2Cl_2, V): 0.70.

Preparation of 10-(Ferrocenylalkyl)-9(10*H*)-acridinone (5a and 5b). Sodium hydride (0.07 g, 2.92 mmol) was added to a solution of 9(10*H*)-acridone (0.26 g, 1.33 mmol) in DMF (50 mL) and the reaction mixture stirred for 30 min at 50 °C. (8-Bromooctyl)ferrocene (0.50 g, 1.28 mmol) was added and the reaction mixture heated under reflux for 24 h. The solvent was removed in vacuo, the residue taken up in CH_2Cl_2, the solution washed with water, the organic layer treated with $MgSO_4$, and the solvent removed in vacuo. Column chromatography of the residue on silica gel (CH_2Cl_2) gave the crude product as the third band. This was further purified on preparative silica plates (2:1:1 CH_2Cl_2−EtOAc−hexane), giving pure **5a** as the second band (0.34 g, 52%). Anal. Calcd for $C_{31}H_{33}ONFe$: C, 75.75; H, 6.76; N, 2.85. Found: C, 75.81; H, 7.08; N, 2.81. ^{1}H NMR ($CDCl_3$, δ): 1.36−1.57 (m, 12*H*, −CH_2−), 1.92 (t, 2*H*, *J* = 8.1 Hz, −CH_2−), 2.33 (t, 2*H*, *J* = 8.1 Hz, −CH_2−), 4.03−4.06 (m, 2*H*, η^5-C_5H_4), 4.08 (s, 5*H*, η^5-C_5H_5), 4.30 (t, 2*H*, *J* = 8.4 Hz, η^5-C_5H_4), 7.28 (ddd, 2*H*, *J* = 15.3, 7.2, 1.2 Hz, acridone *H*), 7.47 (d, 2*H*, *J* = 8.7 Hz, acridone *H*), 7.71 (ddd, 2*H*, *J* = 15.6, 8.4, 1.5 Hz, acridone *H*), 8.58 (dd, 2*H*, *J* = 8.1, 1.5 Hz, acridone *H*). IR (CH_2Cl_2, cm^{-1}): 1630, 1600. $E^{+/0}$ (CH_2Cl_2, V): 0.49. A similar reaction with (11-bromoundecyl)-ferrocene gave **5b** (89 mg, 39%). EI-MS: *m*/*z* 533 (M^+). ^{1}H NMR ($CDCl_3$, δ): 1.17 (t, 2*H*, *J* = 7.2 Hz, −CH_2−), 1.23−1.50 (m, 14*H*, −CH_2−), 2.27 (t, 2*H*, *J* = 7.8 Hz, −CH_2−), 4.00 (t, 2*H*, *J* = 1.8 Hz, −CH_2−), 4.03−4.06 (m, 2*H*, η^5-C_5H_4), 4.08 (s, 5*H*, η^5-C_5H_5), 4.35 (t, 2*H*, *J* = 8.4 Hz, η^5-C_5H_4), 7.25 (ddd, 2*H*, *J* = 16.2, 9, 0.9 Hz, acridone *H*), 7.54 (dd, 2*H*, *J* = 9.3, 0.3 Hz, acridone *H*), 7.73 (ddd, 2*H*, *J* = 16.8, 9.9, 1.5 Hz, acridone *H*), 8.23 (dd, 2*H*, *J* = 9.9, 1.8 Hz, acridone *H*).

Preparation of 2-Ethynylferroceneanthraquinone (6). A solution containing 2-iodoanthraquinone (100 mg, 0.3 mmol), ethynylferrocene (64 mg, 0.3 mmol), 2 mol % $PdCl_2(Ph_3P)_2$/CuI in diisopropylamine (15 mL), and THF (15 mL) was refluxed for 5 h. The reaction mixture was then extracted into CH_2Cl_2, and the extracts were washed with water and treated with $MgSO_4$. The organic extracts were concentrated and chromatographed on silica gel (CH_2Cl_2). The second band gave **6** (86 mg, 69%). Anal. Calcd for $C_{26}H_{16}O_2Fe$: C, 75.02; H, 3.87. Found: C, 74.62; H, 3.72. ES-MS: *m*/*z* 417 (M^+). ^{1}H NMR ($CDCl_3$, δ): 4.28 (s, 5*H*, η^5-C_5H_5), 4.33 (t, 2*H*, *J* = 1.8 Hz, η^5-C_5H_4), 4.57 (t, 2*H*, *J* = 1.8 Hz, η^5-C_5H_4), 7.80−7.86 (m, 3*H*,

(29) Abram, T. S.; Watts, W. E. *Synth. React. Inorg. Met.-Org. Chem.* **1976**, *6*, 31−53.
(30) Bruce, M. I.; Skelton, B. W.; Smith, M. E.; White, A. H. *Aust. J. Chem.* **1999**, *52*, 431−435.
(31) Vlassa, M.; Silberg, I. A.; Custelceanu, R.; Culea, M. *Synth. Commun.* **1995**, *25*, 3493−3501.
(32) Ranatunge-Bandarage, P. R. R.; Robinson, B. H.; Simpson, J. *Organometalllics* **1994**, *13*, 500−510.
(33) PC SPARTAN Plus Version 1.5; Wavefunction Inc., 18401 Von Karman Ave., Suite 370, Irvine, CA 92612, 1998.
(34) Schaftenaar, G.; Noordik, J. H. *J. Comput.-Aided Mol. Design* **2000**, *14*, 123−134.

anthra *H*), 8.27 (d, 1*H*, $J = 8.4$ Hz, anthra *H*), 8.31−8.34 (m, 2*H*, anthra *H*), 8.38 (d, 1*H*, $J = 1.2$ Hz, anthra *H*). IR (CH_2Cl_2, cm^{-1}): 2209 (ν(C≡C)), 1676, 1596 (ν(CO), ν(C═C)). $E^{+/0}$ (CH_2Cl_2, V): 0.71.

Preparation of 1-Ferrocenylanthraquinone (7). A stirred solution of ferrocene (3.7 g, 19.8 mmol) in CH_2Cl_2 (50 mL) was treated with Aldrich Fast Red Salt (10.0 g, 7.4 mmol). The solvent was removed in vacuo and residue purified chromatographically on alumina (hexane). The second band yielded **7** (0.90 g, 31%). Anal. Calcd for $C_{24}H_{16}O_2$; C, 73.49; H, 4.11. Found: C, 73.32; H, 4.07. ^{1}H NMR ($CDCl_3$, δ): 4.12 (s, 5*H*, η^5-C_5H_5Fe), 4.44 (t, 2*H*, $J = 2$ Hz, η^5-C_5H_4), 4.51 (t, 2*H*, $J = 2$ Hz, η^5-C_5H_4), 7.69 (t, 1*H*, $J = 8$ Hz, anthra *H*), 7.74−7.75 (m, 1*H*, anthra *H*), 7.81 (dd, 1*H*, $J = 6$, 3 Hz, anthra *H*), 8.14−8.16 (m, 1*H*, anthra *H*), 8.24−8.26 (m, 1*H*, anthra *H*), 8.30 (dd, 1*H*, $J = 8$, 2 Hz, anthra *H*), 8.33 (dd, 1*H*, $J = 6$, 3 Hz, anthra *H*). IR (CH_2Cl_2, cm^{-1}): 1666, 1578 (ν(CO), ν(C═C)). $E^{+/0}$ (CH_2Cl_2, V): 0.60.

Preparation of (*E*)-2-Ethenylferrocenylanthraquinone (8). A mixture of vinylferrocene (0.16 g, 0.76 mmol), 2-iodoanthraquinone (0.20 g, 0.6 mmol), palladium acetate (10 mg, 6% molar to the aromatic halide), tris(*o*-tolyl)phosphine (25 mg, 10% molar), and 5 equiv of triethylamine (4 mmol) in DMF (35 mL) was heated for 24 h at 80−90 °C. The solution was cooled and filtered, and the solvent was evaporated. Column chromatography on silica gel (CH_2Cl_2) gave an orange band (unreacted vinylferrocene) and then a dark red band **8** (38%, 80 mg). Anal. Calcd for $C_{26}H_{18}FeO_2$; C, 74.64; H, 4.30. Found: C, 74.69; H, 4.79. ^{1}H NMR ($CDCl_3$, δ): 4.17 (s, 5*H*, η^5-C_5H_5), 4.37 (t, 2*H*, η^5-C_5H_4), 4.50 (t, 2*H*, η^5-C_5H_4), 6.82 (dd, 1*H*, $J =$ 16 Hz, vinyl), 7.24 (dd, 1*H*, $J = 16$ Hz, vinyl), 7.75 (d, 1*H*), 7.81 (t, 1*H*), 8.25 (t, 2*H*), 8.32 (d, 1*H*), 8.34 (t, 2*H*). IR (CH_2Cl_2, cm^{-1}): 1672, 1611, 1588 (ν(CO), ν(C═C)). $E^{+/0}$ (CH_2Cl_2, V): 0.53.

X-ray Data Collection and Structure Solution for 3 and 6. Crystal data for **3** and **6** are given in Table 4. Both compounds were recrystallized from CH_2Cl_2 with pentane diffusion as dark red and orange plates, respectively. Data were collected at 158(2) K for **3** and 168(2) K for **6** on a Bruker SMART CCD diffractometer and processed using SMART[35] with empirical absorption corrections applied using SADABS.[36] The structures were solved using SHELXS[37] and refined by full-matrix least squares on F^2 using TITAN2000[38] and SHELXL-97.[37] All non-hydrogen atoms were assigned anisotropic temperature factors, with hydrogen atoms included in calculated positions. For **3** the correct choice of absolute structure was confirmed by refinement of the Flack parameter (0.050(17)).

Table 4. Crystal Data and Structure Refinement Details for 3 and 6

	3	6
empirical formula	$C_{25}H_{18}NOFeI$	$C_{26}H_{16}O_2Fe$
fw	531.15	416.24
cryst syst	monoclinic	monoclinic
space group	*Cc*	$P2_1/n$
abs coeff, mm^{-1}	2.288	0.875
final *R* indices ($I > 2\sigma(I)$)	R1 = 0.0189, wR2 = 0.0421	R1 = 0.0587, wR2 = 0.0880
final *R* indices (all data)	R1 = 0.0200, wR2 = 0.0423	R1 = 0.1917, wR2 = 0.1026
goodness of fit on F^2	1.025	0.877
temp, K	158(2)	168(2)
wavelength, Å	0.710 73	0.710 73
unit cell dimens		
a, Å	8.040(2)	11.772(7)
b, Å	19.437(6)	8.311(6)
c, Å	13.085(4)	18.336(9)
β, deg	98.359(4)	100.16(2)
V, Å^3	2023.2(10)	1765.8(18)
Z	4	4
density (calcd), Mg/m^3	1.744	1.566
F(000)	1048	856
no. of rflns collected	6504	7527
no. of indep rflns	2463 (*R*(int) = 0.0227)	3351 (*R*(int) = 0.1033)

There is some evidence of disorder for the atoms C(15) and C(16) in the structure of **6**, with a number of small peaks in the final difference Fourier map located close to the C≡C bond. However, no clear path to resolving the disorder was apparent, and it was not investigated further. An additional indication of the problem is given by the unusually short C(15)−C(16) bond distance, and this value should be viewed with caution.

Acknowledgment. We thank the University of Otago for financial support, the Marsden Fund, Royal Society of New Zealand, for partial support, Prof. W. T. Robinson (University of Canterbury) for X-ray data collection, Dr. A. N. Rieger (Brown University) for recording the ESR spectrum, and Dr. K. Gordon for helpful discussions. Compound **8** was originally prepared by Mr. B. Dana in these laboratories. We also thank Dr. M. Murata (University of Tokyo) for prior notification of results and preprints.

Supporting Information Available: Tables giving final positional and equivalent thermal parameters, all bond lengths and angles, anisotropic thermal parameters, and hydrogen positional and isotropic displacement parameters for both compounds. This material is available free of charge via the Internet at http://pubs.acs.org.

OM020747T

(35) SMART CCD Software; Bruker AXS, Madison, WI, 1994.
(36) SADABS (correction for area detector data); Bruker AXS, Madison, WI, 1997.
(37) Sheldrick, G. M. SHELXS: A Program for the Solution of Crystal Structures from Diffraction Data; University of Göttingen, Göttingen, Germany, 1990. Sheldrick, G. M. SHELXL-97: A Program for the Refinement of Crystal Structures; University of Göttingen, Göttingen, Germany, 1997.
(38) Hunter, K. A.; Simpson, J. TITAN2000: A Molecular Graphics Program To Aid Structure Solution and Refinement with the SHELX Suite of Programs; University of Otago, Otago, New Zealand, 1999.